Methodological framework for assessing the sustainability of electric passenger fleets: Application to the Egadi Archipelago

Applied Energy 401 (2025) 126679

Contents lists available at ScienceDirect

Applied Energy

journal homepage: www.elsevier.com/locate/apen

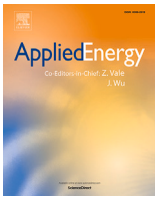

Methodological framework for assessing the sustainability of electric passenger fleets: Application to the Egadi Archipelago

Francesco Balestrieri [a,*], Alessandro Brusasco [b], Matteo Melchiorre [a], Mauro Bonfanti [a], Stefano Mauro [a]

[a] Politecnico di Torino, Department of Mechanical and Aerospace Engineering, Turin, 10129, Italy
[b] Politecnico di Torino, Department of Applied Science and Technology, Turin, 10129, Italy

HIGHLIGHTS

- Parametric evaluation of fleet electrification.
- Reduction in operating costs by switching to electric solutions.
- Comparative analysis of hydrogen-electric hybrid solutions.
- Environmental consequences of different energy solutions and blends.
- Sustainability implications and retrofit roadmap to 2050.

ARTICLE INFO

Keywords:
Naval passenger transportation
Hydrofoil vessels
Electrification
Hydrogen propulsion
Parametric model
Emission reduction
Cost estimation

ABSTRACT

Maritime transport is essential for island communities but remains highly dependent on fossil fuels, posing significant economic and environmental risks, especially in ecologically sensitive regions. This study introduces a novel and adaptable methodology for the preliminary assessment of passenger fleet electrification, using the Egadi Archipelago (Italy) as a case study. A generalisable parametric model was developed to evaluate the techno-economic feasibility and environmental impact of converting the current fast-ferry fleet to battery-electric, hybrid electric-hydrogen, or pure hydrogen propulsion systems. The model estimates energy consumption, emissions, capital investment, and operational costs across long-term planning horizons up to 2050. Findings indicate that electrification can achieve CO_2 reductions of 28 % with gray hydrogen and up to 65 % with green hydrogen, alongside operational cost savings between 40 % and 58 % depending on the energy source considered. The analysis also highlights the substantial renewable energy potential within the archipelago, supporting the goal of zero-impact electric fleet operation. This work offers valuable insights for policymakers, naval architects, and operators in advancing sustainable maritime transport in island and coastal regions.

1. Introduction

In recent years, the imperative to reduce pollutant emissions in the maritime industry has gained increasing urgency. Since 2011, the International Maritime Organization (IMO) has implemented the first globally binding measures aimed at improving ship energy efficiency and curbing greenhouse gas (GHG) emissions, which are among the primary contributors to global temperature rise [1–5]. The IMO's initial strategy, adopted in 2018, established an ambitious framework to eliminate GHG emissions from international shipping by the end of the century. Specifically, it set targets to reduce carbon intensity by at least 40 % by 2030 (and 70 % by 2050), and to cut total annual GHG emissions by 50 % by 2050, relative to 2008 levels. In response to these objectives, a range of strategies has been developed, including the adoption of alternative fuels and electric propulsion systems [6–9], optimization of navigational routes [10], integration of digital twin frameworks [11] and machine learning models [12] into operations, as well as the design of novel hull forms and propellers [2,13]. Among these approaches, vessel electrification has emerged as a transformative trend, offering significant environmental and operational benefits for both large and

* Corresponding author.
Email addresses: francesco.balestrieri@polito.it (F. Balestrieri), alessandro.brusasco@polito.it (A. Brusasco), matteo.melchiorre@polito.it (M. Melchiorre), mauro.bonfanti@polito.it (M. Bonfanti), stefano.mauro@polito.it (S. Mauro).

https://doi.org/10.1016/j.apenergy.2025.126679
Received 21 March 2025; Received in revised form 25 July 2025; Accepted 20 August 2025
Available online 4 September 2025

small craft [14,15]. However, due to the current limitations in battery storage, particularly in terms of cost, volume, and mass, hybrid architectures remain the predominant solution for larger vessels. Within this context, hydrogen is increasingly recognized as a pivotal energy carrier for maritime decarbonization [16,17]. Mallouppas [18] reviews the latest literature on renewable energy sources and alternative fuels for the shipping industry, recognising the important role of fuel cells (FCs) in reducing fuel consumption. Elkafas [19] reviews various FC technologies and international research initiatives in the shipping sector, outlining the advantages and constraints of each solution. Similarly, Fu [20] provides an in-depth analysis of FC-based hybrid architectures, focusing on machinery costs and system configurations for cargo vessels. Sürer [21] highlights ongoing projects related to the use of Proton-Exchange Membrane Fuel Cells (PEM-FC) in maritime transport, emphasizing the sustainable and environmentally positive aspects of hydrogen derived from seawater. Korkmaz [22] assesses the environmental and economic impact of replacing diesel generators on a large tanker with hybrid FCs and battery systems. He identifies the most effective configurations, showing that CO_2 emissions could be reduced by up to 50 % and that electricity production costs could be as low as 0.181 $/kWh. Against this background, recent studies have explored several critical aspects of the transition toward full-electric or hybrid ferries. These include the assessment of fleet replacement options [23,24], financial modelling of hydrogen-powered systems [25] and batteries [26], and performance optimization of vessels equipped with FCs and batteries [27,28]. Rodseth et al. [29] further investigate the optimal composition of a zero-emission fleet, accounting for both vessel deployment and charging infrastructure requirements. Wang [26] comparatively assesses the environmental and economic performance of battery-powered vessels using Life Cycle Analysis (LCA) and Life Cycle Cost Assessment (LCCA) to quantify the benefits of replacing marine diesel engines and generator sets with batteries and electric motors. Miretti [24] describes the benefits of converting waterbuses in the city of Venice to hybrid power, addressing the relevant benefits that can be derived from retrofitting combustion engine ferries. Sundvor et al. [23] model the electrification of Norwegian passenger vessels by leveraging national fleet data to estimate power demands and determine the lowest-emission solution for each route, thereby contributing to a practical fleet renewal strategy. In a complementary study, Chiche et al. [28] present a case analysis of a Swedish rescue vessel retrofitted with FC propulsion.

While the aforementioned studies provide valuable insights into zero-emission maritime fleets, several critical gaps persist in the existing literature. First, prior research has predominantly focused on large vessels, a logical emphasis given their disproportionate contribution to maritime emissions, the regulatory attention they receive, and the relative abundance of data. However, small- to medium-sized vessels remain comparatively under-explored, despite their prominent role as emitters in coastal zones and their greater suitability for electrification. Moreover, these vessels exhibit high operational heterogeneity, which complicates the collection of representative data and limits the generalizability of existing models. Second, recent studies rely on geographically specific datasets and lack the scalability necessary for broader policy or design implications. Additionally, no existing study to date has systematically examined the combined deployment of FC and battery systems, particularly the dynamic alternation between the two energy supply systems, while also evaluating long-term emissions trajectories, lifecycle capital and operational expenditures (CAPEX and OPEX). To address the identified research gaps, this study presents a scalable and computationally efficient framework for evaluating the electrification of passenger ship fleets, with a specific focus on small- to medium-sized vessels. The model enables extrapolation from a single representative vessel to the fleet level, capturing a continuum of electric–hydrogen hybrid propulsion configurations and diverse operational scenarios. It incorporates technical specifications and performance estimates for both displacement and planing hulls, including hydrofoil designs. The framework supports a comprehensive parametric analysis across key design variables (i.e., FC and battery sizing, energy management strategies, and routing profiles) while integrating cost modelling (CAPEX and OPEX) and emissions (CO_2, NO_x and particulate matter) forecasting. Here, CAPEX refers to the purchase cost of the required components, excluding installation and integration, while OPEX is the estimated cost of energy needed to complete the routes. Since the modelled powertrains produce no emissions during use, their environmental impact is calculated based on the CO_2 generated at the energy production source. Additionally, uncertainty quantification is employed to assess the robustness of long-term techno-economic projections under varying technological and operational assumptions. The Egadi Archipelago is selected as a case study due to its urgent need for maritime decarbonization to protect marine biodiversity and improve transport services. A hydrofoil was chosen as the reference vessel, reflecting its current use and high suitability for efficient electric propulsion systems [30,31]. Overall, the tool offers a decision-support environment for fleet decarbonization, providing actionable insights into the trade-offs and benefits of hybrid energy systems. This work contributes to the advancement of sustainable maritime transport by delivering an integrated methodology for the techno-economic and environmental evaluation of zero-emission ferry systems.

The remainder of this paper is organized as follows: in Section 2 the scenario of the Egadi Archipelago is described, including its naval routes, current fleet and the role of the fleet electrification; in Section 3 the novel design tool is presented, providing a description of its architecture, numerical models, assumptions, parameters and output; in Section 4 the results regarding the electrification of the fleet operating in the Egadi Archipelago are discussed in terms of a techno-economic-environmental point of view, reporting also uncertainty metrics; Section 5 investigates the long-term results of a retrofit plan, comparing the results of different scenarios up to 2050 and addressing the price projections of the involved systems and energy sources; then, in Section 6 some conclusions and further works are reported.

2. Case study: the Egadi Archipelago waterborne scenario

Egadi Islands, shown in Fig. 1, are characterized by their limited geographical area, small populations, and fragile ecosystems. For this reason, they require tailored transportation solutions to balance environmental preservation with the mobility needs of residents and tourists [32].

Fig. 1. Egadi islands map.

Located off the western coast of Sicily, Italy, the Archipelago includes the islands of Favignana, Levanzo, and Marettimo. It is renowned for its rich biodiversity and is home to the largest Marine Protected Area (MPA) in Europe, encompassing approximately 53992 hectares of marine environment and 74 km of coastline [32]. The archipelago has a resident population of, on the 1st of January 2021, 4448 inhabitants [33], primarily distributed across the islands of Favignana, Levanzo, and Marettimo, with the majority residing on Favignana (3407 inhabitants).

During peak tourist season, this number swells significantly, placing additional strain on the local transport infrastructure. In fact, due to the great vocation for tourism, peaks of 64100 inhabitants [33] are reached during the summer (see Fig. 2), which is almost fifteen times the number of residents (see Fig. 3).

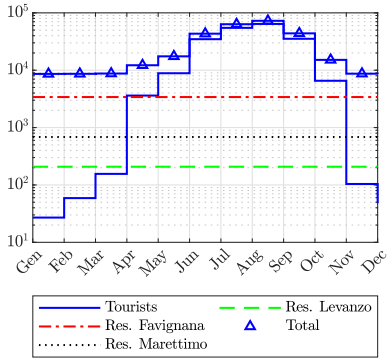

Fig. 2. Number of people in the archipelago. Residents: 3407 in Favignana, 684 in Marettimo and 208 in Levanzo [33].

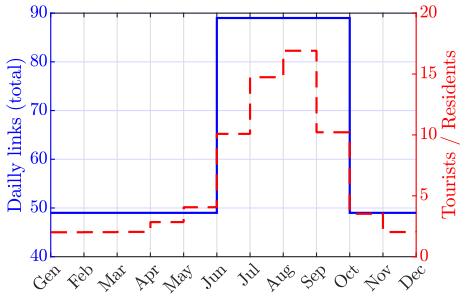

Fig. 3. Number of daily routes on a monthly base and tourist over residents monthly ratio.

The significant human pressure during the summer months, combined with the complexity of managing the territory and its resources, creates a challenging maritime transport context [32]. This is linked to the need to protect the environment, which has led to the establishment of a marine protected area. The creation of a marine reserve dates back to 1991 [32], and was intended to prevent the use of areas adjacent to the archipelago for the installation of oil platforms. The MPA aims to conserve or restore the most significant natural features of the marine environment, protect marine resources, educate the public about marine habitats, support scientific research, enhance the protection of local archaeological sites, and promote socio-economic activities in the area. Improving the maritime sector is closely related to the MPA's goals, as the impact of maritime transport on marine ecosystems is part of the EU Marine Strategy Framework Directive [34].

2.1. Routes and operational profile of the Egadi fleet

Since the whole archipelago is included in the marine reserve, the routes connecting the islands to each other and to the mainland must also comply with environmental regulations. Consequently, vessels contribute to air and water pollution, greenhouse gas emissions, and noise, adversely affecting the MPA and environmental health. Fast transport is primarily provided by the private company Liberty Lines [35], whose fleet includes hydrofoils and planing boats, all powered by diesel engines. The company routes create a dense network of daily connections, enabling travel between the islands in less than an hour. The number of daily trips fluctuates with the seasons, with a noticeable increase from June to September, related to the rise in tourist numbers, as shown in Fig. 3. Due to the short distances between islands (see Table 1), routes often include multiple stops to reduce the number of active vessels needed, despite a high number of daily trips. This necessitates the reconstruction of a detailed timetable to estimate fuel consumption and determine boat energy requirements. Fig. 4 shows the reconstructed schedule based on Liberty Lines' timetable [35], indicating the need for at least 5 operative vessels during summer operations, reduced to 3 during winter. These vessel will be used for estimating annual emissions and operational costs.

Table 1
Distances between islands of Egadi archipelago (in nautical miles, nm) and expected time to reach straight one each other.

Course	Distance	Expected time
Trapani - Favignana	10.1 nm	25–30 min
Trapani - Levanzo	10.3 nm	25–30 min
Trapani - Marettimo	21.8 nm	45–60 min
Favignana - Levanzo	3.3 nm	10–15 min
Favignana - Marettimo	15.6 nm	30–40 min
Favignana - Marsala	13.9 nm	30–40 min
Levanzo - Marettimo	12.4 nm	25–30 min

2.1.1. The admiral 250

Liberty Lines fleet includes 19 hydrofoils, 5 planing mono-hulls, and 5 planing catamarans [35]. These boats, built between the late 1990s and 2019, are all powered by diesel engines.

To standardize the fleet and compare model results with a recent vessel, a hydrofoil model Admiral 250 (see Fig. 5), built in 2019, is considered as a reference. Specifications for this vessel [35] are provided in Table 2. To calculate fuel consumption (F) for this vessel on the routes shown in Fig. 4, estimates are made route by route. The fuel consumption is computed as:

$$F = SFC \int P_B \, dt_r \tag{1}$$

where SFC denotes the Specific Fuel Consumption, as reported in Table 2, and P_B and t_r represent the estimated engine-delivered power (as described in Section 3) and the route duration, respectively. Note that the integral of P_B over the time interval t_r corresponds to the energy required to complete the route.

Fig. 6 displays the results of this estimation, showing variations in fuel requirements attributable to the frequency of trips on different routes. During summer, 20.8 tons of diesel fuel are required daily for inter-island travel, while in winter this drops to 11.0 tons, overall affecting the archipelago's flora and fauna.

2.2. Diesel engine propulsion

The Liberty Lines fleet is powered by Internal Combustion Engines (ICE), specifically diesel engines. These engines serve multiple roles, including main propulsion and auxiliary power generation [2]. Diesel engines operate on the principle of compression ignition [36], in which air is compressed to high pressure and temperature, causing the injected fuel to ignite spontaneously. This combustion process generates torque by driving the piston, which is mechanically linked to the main driveshaft, thereby delivering power to the propulsion system. Modern marine diesel engines are well-regarded for their ability to produce high torque at low rotational speeds (RPM), making them particularly well-suited for the rigorous operational demands of naval vessels [37]. They are engineered to endure harsh maritime environments, including high salinity, humidity, and significant temperature variations, and are designed for extended continuous operation. Power outputs vary widely, ranging from a few hundred kilowatts in small vessels to several megawatts in large ships. Technological advancements such as turbocharging and intercooling have significantly improved both power density and thermal efficiency, with some engines achieving efficiencies

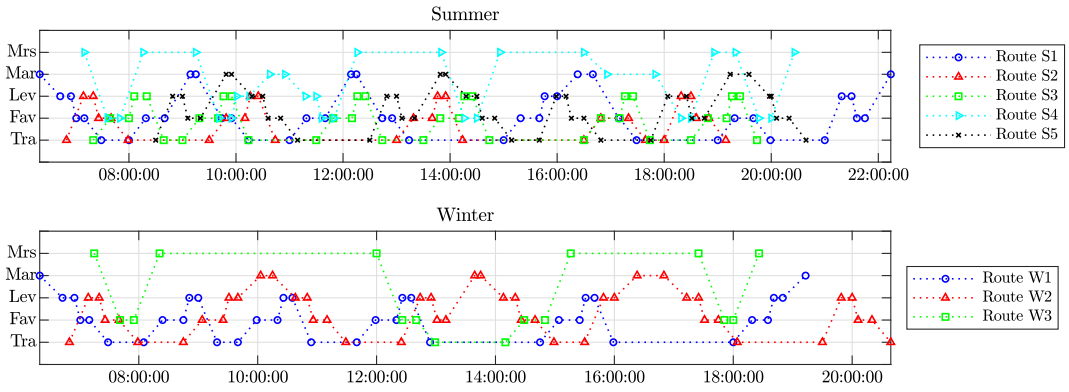

Fig. 4. Recreation of seasonal daily routes timetable.

Fig. 5. Reference boat - Admiral 250.

exceeding 50 % [38]. To meet the International Maritime Organization (IMO) Tier III emissions standards—such as those applicable to the CatMarine 3516 CHD—nitrogen oxide (NO_x) emissions must be reduced by approximately 70 %. These regulatory requirements [3,39] have driven the adoption of emissions-reducing technologies such as exhaust gas recirculation (EGR), selective catalytic reduction (SCR), and the development of alternative fuels. These systems are instrumental in reducing both NO_x and sulfur oxide (SO_x) emissions, thereby enhancing the environmental performance of diesel engines [38]. In response to increasing environmental concerns, modern vessels are progressively incorporating hybrid propulsion systems that integrate electric motors. These configurations improve fuel efficiency and reduce emissions. However, a truly zero-emission engine remains unfeasible due to the unavoidable byproducts of the combustion process. To estimate pollutants released by a diesel engine, the emissions of the Admiral 250 fleet

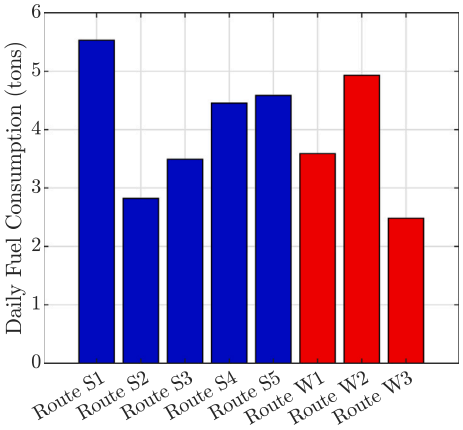

Fig. 6. Daily consumption over different routes and seasons.

Table 2
Reference boat specifications.

Parameter	Value
Model	Admiral 250
Category	Passenger ship
Number of passengers	215
LOA	31.7 m
Beam	4.2 m
Max displacement	147 tons
Max speed	35 ktn
Cruise speed	32 ktn
Engine	CatMarine3516CHD
Power per engine	2000 kW
Number of engines	2
Engine Weight	10,447 kg
Specific Fuel Consumption	0.1985 kg/kWh

Table 3
Tier III emission standards from EPA.

CO (c_{CO})	HC + NOx (c_{HC+NO_x})	PM (c_{PM})
5 g/kWh	5.8 g/kWh	0.11 g/kWh

equipped with CatMarine 3516 CHD engines are reported. The emitted pollutants are computed as follows:

$$e_{CO,HC+NOx,PM} = \sum_{i=1}^{Nr_{S,W}} c_{CO,HC+NOx,PM} \int P_{B_i} dt_{r_i}$$
$$e_{CO_2} = \sum_{i=1}^{Nr_{S,W}} c_{CO_2} Fuel_i \quad (2)$$

where $c_{CO,HC+NOx,PM}$ is the emission standard limit, P_i and t_{r_i} are respectively the power demand and the required time over the i-th route, $Nr_{S,W}$ is the number of routes in summer or winter, and $e_{CO_2,CO,HC+NOx,PM}$ is the computed emitted pollutant. Emissions are then calculated using consumption data from Fig. 6, Tier III standard levels (Table 3), and a CO_2 emission coefficient (c_{CO_2}) of 2.778 kg/Kg_{Fuel} [40].

Fig. 7 illustrates the significant CO_2 and other emissions produced, underscoring the need to reduce anthropogenic pressure on this delicate ecosystem.

2.3. Transition to full electric propulsion

2.3.1. Electric propulsion

As the demand for more sustainable and versatile maritime operations increases, electric propulsion systems are becoming an essential component in both new ship designs and retrofits [41]. Electric systems

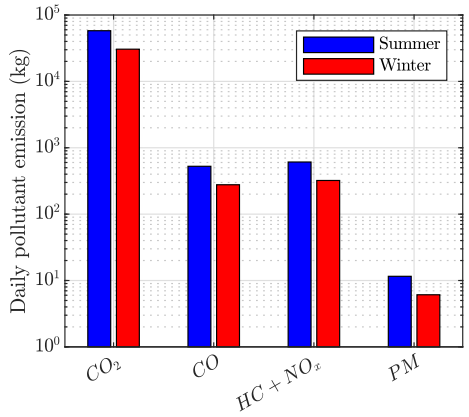

Fig. 7. Fleet daily emissions estimate.

are primarily used for propulsion, providing a cleaner and quieter alternative to traditional diesel engines. Modern electric motors achieve efficiencies exceeding 90 % [42], minimizing energy loss and optimizing fuel consumption when combined with generators [43]. Various types of electric motors are employed in naval applications, including synchronous motors, asynchronous (induction) motors, and permanent magnet motors. Each type possesses unique advantages [41]; for instance, synchronous motors offer high efficiency and precise speed control, while induction motors are known for their robustness and reliability. Electric motors also generate significantly less acoustic noise and vibration compared to traditional engines, primarily due to their reduced number of moving parts [42]. This is particularly valuable in areas where marine fauna need to be protected, such as the Egadi MPA. Furthermore, the lower number of moving parts translates to lower maintenance requirements and higher reliability. Combined with advanced monitoring and diagnostic systems, this reduces the risk of unexpected failures and extends the operational lifespan of the propulsion systems. The effectiveness of electric propulsion is closely tied to advancements in electric energy storage solutions [14], such as lithium-ion batteries and supercapacitors. However, these storage systems often struggle to meet the operational capacity requirements. A promising alternative to batteries is hydrogen [16,19] coupled with FC. Using hydrogen in combination with FCs (like PEMFCs) enables extended operations of full-electric propulsion systems, overcoming the drawbacks associated with batteries.

2.3.2. Hydrofoil technology

In the context of maritime electrification, where storing large amounts of energy remains a key challenge, hydrofoils offer a significant technological advantage. By lifting the hull out of the water at high speeds, hydrofoils drastically reduce hydrodynamic drag [30,31], thereby lowering power demand and reducing both energy consumption and storage requirements. This efficiency gain makes them particularly suitable for integration with electric and hybrid propulsion systems. Many recent electric vessel designs incorporate hydrofoils, highlighting the growing synergy between these technologies. To be effective, hydrofoils require a takeoff phase during which sufficient speed is achieved to generate lift and elevate the hull [30]. When combined with renewable energy sources, hydrofoils further enhance environmental performance, enabling net-zero CO_2 emissions during operation [15]. This study builds upon these advantages, integrating hydrofoil dynamics to enhance the transition of fleets toward green propulsion.

3. Parametric model for electric fleet assessment

The developed model aims to estimate the effects of electrifying a fast hydrofoil passenger ferry. By defining basic boat parameters, key route features, and specific coefficients, the model provides estimates of propulsion costs and emissions for the whole fleet. The electrification process results in a fleet that emits zero pollutants during operation while maintaining the same performance (i.e., the required operational speed) as the original fleet. To achieve this zero-emission goal, only electric motors are considered for the propulsion system, and the energy storage can range from batteries to hydrogen, encompassing all intermediate options.

3.1. Powertrain architecture

To design a hybrid hydrogen-battery energy storage system, it is necessary to determine the required energy contribution from each energy carrier. This is achieved through a blending factor, defined as follows:

$$\gamma = \frac{BF}{1 + BF} \tag{3}$$

where BF is the ratio between hydrogen and battery capacity. A γ value of 0 represents a full battery storage, while 1 represents a full hydrogen storage. Moreover, this model does not specify a particular hybrid powertrain architecture: both parallel and serial configurations of batteries and FCs are considered. Despite the model focusing on the overall energy requirements and not delving into specific architectural changes, it's possible to generally state that the choice between a parallel or serial FC-battery architecture depends on the selected blending factor. A small hydrogen capacity with its corresponding FC can potentially be used as a range extender, storing excess energy in a larger battery pack for later use. On the other hand, if the hydrogen capacity and FC power are increased to match or exceed the engine power demand, a parallel architecture might be more suitable. This configuration is particularly well-suited for cruise regimes where the FC can operate at a relatively constant point, maximizing efficiency. Additionally, a parallel architecture can potentially improve overall efficiency compared to a serial one, as there is no energy dissipation associated with recharging the battery from the FCs.

3.2. Model structure and assumptions

The code, as shown in Fig. 8, is structured in a double loop architecture, where the outer loop works to reduce the weight residual between one iteration and the previous one, while the inner loop sizes the powertrain to fit requirements given by the selected scenario. Specifically, the distinction between the inner and outer loops is emphasized by respectively a blue and red dotted lines which enclose the loop steps.

3.2.1. Modelling hydrofoil resistance

As shown in Fig. 8, the design algorithm begins by estimating the vessel's drag, which directly influences both engine power requirements and overall energy consumption. The drag is assessed by combining experimental data from Ref. [44] with general hydrodynamic trends reported in [30,31]. Using a reference cruise speed (V_{cruise}) of 32 knots, the data from Ref. [44] closely match the typical drag characteristics of hydrofoil vessels described in [30]. To generalize the drag behaviour across varying speeds, the ratio between the drag at any given speed and the drag at cruise speed is required. However, due to limited available data, this ratio cannot be directly scaled from the experimental dataset. To address this, the model assumes a lift-to-drag ratio (L/D) for the hydrofoil. Despite its approximate nature, this assumption yields results consistent with experimental observations, as discussed in Section 3.2.3. Given that vertical equilibrium must be maintained during operation, the lift force is assumed equal to the vessel's weight. Based on the adopted L/D value, the corresponding drag force at cruise speed (D_{cruise}) can be derived. This, in turn, allows the computation of a complete drag–speed curve using the normalized drag trends as a function of normalized velocity, as illustrated in Fig. 9.

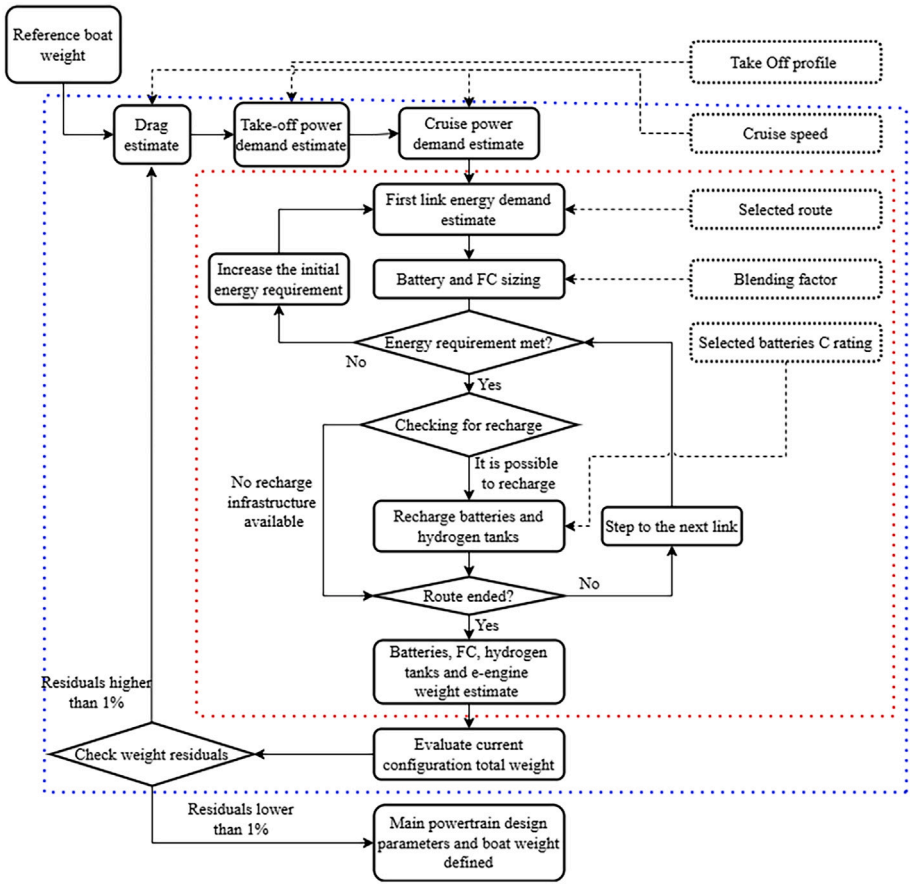

Fig. 8. Model scheme.

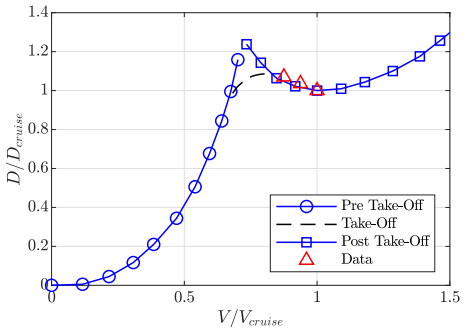

Fig. 9. Normalized drag as the change of normalized boat speed [30,44].

3.2.2. Propeller and propulsion system

Boat resistance is needed to obtain the effective delivered power $P_E = DV$, and an estimate of the engine brake power [45,46] (P_B). The engine brake power is subject to different losses, mainly due to the propeller efficiency, its interaction with the hull and the transmission system. The propulsive efficiency (η_{prop}), accounts for all these losses and can be computed as follows:

$$\eta_{prop} = \frac{P_E}{P_B} = \eta_H \eta_O \eta_R \eta_S \tag{4}$$

where η_H is the hull efficiency, η_O is the open water propeller efficiency, η_R is the relative rotative efficiency, and η_S is the shaft efficiency. No data are available on the propeller which equips the Admiral 250, so a η_O has been computed considering a parameterized five blades Wageningen B-Series propeller and the propeller matching procedure described in [45,47], which gives a $\eta_O = 0.72$ for the design condition. Fig. 10 shows the propeller performance as function of the advance ratio (J), its torque (K_q) and thrust (K_t) coefficients and the matching with the boat characteristics defined by the ship thrust coefficient ($K_{t_{ship}}$) as described by Ref. [45,47], whose results are in line with an efficient propeller [45,47–49]. While the value of η_O has been computed based on a real propeller shape, other efficiencies have been assumed considering a conservative approach, so $\eta_H = 1.02$ which is smaller than conventional displacement hull values [45,46], $\eta_R = 1$ as reported by Ref. [46] a good approximation for initial design evaluations and $\eta_S = 0.96$ which is considered a representative value for a shaft that includes a gearbox [46].

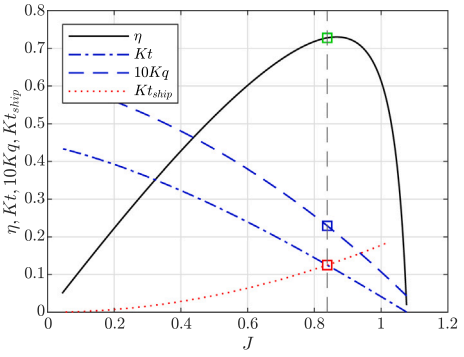

Fig. 10. Propeller characteristics, from a five blades Wageningen B-Series propeller.

3.2.3. Hydrofoil efficiency and cruise power demand

As previously stated, the lift-to-drag ratio (L/D) has been fixed in the model. To determine an appropriate value for this ratio, an iterative approach was adopted. This involved testing a range of plausible L/D values and comparing the resulting model predictions against experimental data provided by Ref. [44], specifically in terms of power demand across various speeds and sea state conditions, representative of the vessel's typical operating environment. The results of this analysis are presented in Fig. 11. As shown, the tested L/D values ranged from 10 to 25, representing, respectively, very low and relatively high hydrodynamic efficiency for a surface-piercing vessel [30].

Fig. 11 displays three distinct curves and a shaded region, representing the following: the computed brake power P_B (blue), the P_B calculated considering only the propeller efficiency (red), and the effective power P_E (gray). The shaded area indicates the range of P_B values as the propeller efficiency, η_{prop}, varies between 0.6 and 0.8. Based on the reported curves and the expected brake power at cruise speed under typical sea state conditions, a value of $L/D = 17$ was selected. This value yields a brake power demand consistent with the expected operating value of 2046 kW, as indicated by the upper dotted line in Fig. 11. It is important to note that this value is significantly higher than the experimentally measured brake power under calm water conditions, which is 1759 kW (highlighted by the lower dotted line in Fig. 11).

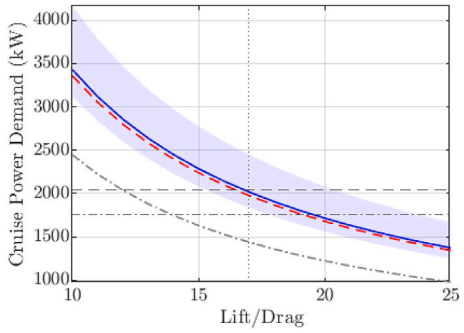

Fig. 11. Cruise power demand as function of the hydrofoil efficiency.

3.2.4. Take-off phase

In order to consider all operational phases and properly size the engine, the take-off (TO) of the vessel has been accounted for. This phase accounts for all the operations which are not part of the cruise, so no distinction has been made between the undocking and in port operations and the acceleration that leads to the effective take off, since all of them have been described in a single operation profile. The TO profile, reported in Fig. 12, has been assumed, since no data are available regarding the effective time required to leave the harbor dock and to reach the cruise speed.

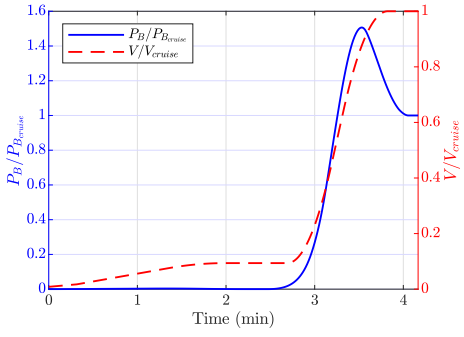

Fig. 12. Normalized power and speed during take-off.

As illustrated in Fig. 12, the power demand exhibits a peak just before reaching the cruise speed when the vessel is lifting from the water. Indeed, despite its minimal contribution to the overall energy demand, the TO phase is relevant to define the peak brake power demand during the operations. However, the TO contribution to the overall energy demand becomes negligible (less than 5 %) when the route length increases over 20 nautical miles, as reported by the trend in Fig. 13. The reported results have been computed using this model on the routes of the Egadi Archipelago. The trend obtained by interpolating these data is comparable to the one reported in [50] which has been obtained for a T-shape fully submerged hydrofoil.

3.2.5. Energy storage sizing

Once the power demand across different speeds has been determined, the energy storage can be sized based on the route energy requirements (E_{req}). E_{req} can be computed as follows:

$$E_{req} = \int P_B dt \tag{5}$$

and is also equivalent to:

$$E_{req} = H_2 LHV_{H_2} \eta_{FC} + B\eta_B + R \tag{6}$$

where H_2 is the mass of hydrogen stored in tanks, LHV_{H_2} is its lower heating value, η_{FC} and η_B are respectively the FC and batteries efficiency, B is the battery capacity and R is the energy recharged (both hydrogen and batteries if possible) during operations. The hydrogen mass and the battery capacity are computed as follows:

$$H_2 = \frac{E^*_{req}}{LHV_{H_2}\eta_{FC} + \frac{LHV_{H_2}}{BF}\eta_B} \tag{7}$$

$$B = \frac{E^*_{req}}{BF\eta_{FC} + \eta_B} \tag{8}$$

Then, the power of the FC is calculated accordingly:

$$P_{FC} = P_{B_{cruise}} \frac{H_2 LHV_{H_2} \eta_{FC}}{E^*_{req}} \tag{9}$$

where $P_{B_{cruise}}$ is the brake power during the cruise phase.

The calculation of FC and battery capacities follows an iterative process that incorporates the possibility of recharging the energy storage systems under specific operational conditions. In the Egadi case study, recharging is permitted only when the vessel docks in Trapani for durations exceeding 15 min. The inner loop of the model begins by evaluating the energy required to complete the first leg of the route, denoted as E^*_{req}. Based on this requirement and the specified blending factor, an initial estimate of the energy storage capacity and fuel cell power output (P_{FC}) is calculated. A verification step follows to determine whether

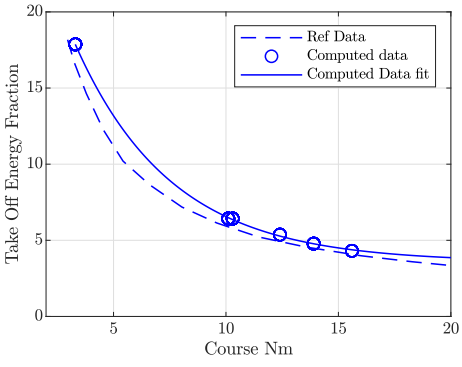

Fig. 13. Take off overall energy fraction as function of the route length.

the estimated storage capacity is sufficient to meet the energy demand for that segment. If the condition is satisfied, the model proceeds to assess the potential for recharging at the scheduled stop, updates the available energy accordingly, and continues to the next segment of the route. This process is repeated iteratively until the full route is evaluated. If, at any point, the available energy is found to be insufficient for completing a segment, the storage capacity is increased by a fixed increment (set to 1 % of the previous value), and the inner loop restarts from the beginning. This adjustment may be triggered by any segment, not only the first, and in such cases, energy consumption must be recomputed for the entire route. Since the model accounts for intermediate recharging opportunities, the time required for these operations must also be considered. For hydrogen refueling, it is assumed that whenever the recharging conditions are met, the hydrogen tanks can be completely refilled. For batteries, however, the recharge amount depends on the duration of the stop (t_{R_i}) and the battery recharge rate (C), which indicates the maximum rate at which the battery can be charged or discharged relative to its total capacity. The energy recharged is then calculated as:

$$R = \sum_{i=1}^{Nr_R} (\min(C B t_{R_i}; B - B_i)\eta_B + (H_2 - H_{2_i}) LHV_{H_2}\eta_{FC}) \quad (10)$$

here Nr_R is the number of links during the route where is possible to recharge and B_i and H_{2_i} are respectively the battery and hydrogen residual capacity before the $i-th$ recharge. Higher the C rate, faster the battery can be recharged/discharged and vice versa. It is worth noting that recharging at high C-rates can lead to energy losses. However, these effects have not been considered in this model, as they depend on specific battery characteristics and external conditions, which are beyond the scope of a preliminary-level assessment tool.

3.3. Weight estimation and iterative refinement

When the inner loop iteration ends, all main parameters of the energy storage compartment are defined and the new overall boat weight can be estimated based on them. Components that affect the weight estimate are: the engine, batteries, the hydrogen tanks and the FCs. Their weight is computed by means of coefficients, see Table 4, provided by literature or derived from manufacturers' catalogs [51], such as in case of the electric motor weight, whose trends, in Fig. 14, were derived from data collected on high voltage motors.

Table 4
Mass estimate coefficients.

Mass coefficient		Value
Engine (see Fig. 14)	m_{p1}	2.115 kg/kWh
	m_{p2}	2026 kg
Battery [52]	m_b	8.33 kg/kWh
Fuel cells [19]	m_{fc}	3.61 kg/kW
Hydrogen tanks [53]	m_t	15 kg/kgH_2

The overall mass estimate was obtained by adding all these single components' contributions to the reference boat displacement while removing its current engines weight. The overall mass estimate (M) is computed as:

$$M = M_{or} - M_{ICE} + (m_{p1}P_{eM} + m_{p2}) + m_b B + m_{fc}P_{FC} + m_t H_2 + H_2 \quad (11)$$

In this expression, M_{or} represents the reference boat displacement, and M_{ICE} denotes the weight of the original internal combustion engine. The coefficients m_*, provided in Table 4, are used to calculate the weights of the individual system components. P_{eM} denotes the electric motor power, estimated based on the maximum power demand derived from the modelling of the take-off phase, as described in Section 3.2.4. Obviously this formulation is raw, but it takes into account all main contributions in the mass prediction. The main uncertainty comes out from

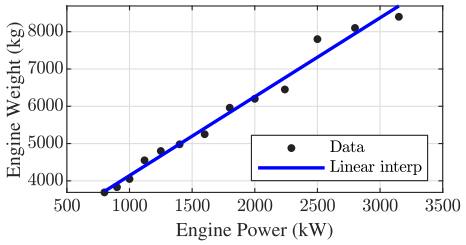

Fig. 14. Engine weight coefficients estimate. Linear fitting, $m_{p1}P_{eM} + m_{p2}$, between power and weight.

structural variations of the boat due to the configuration changes. This kind of estimate goes beyond the simple conceptualization of a boat refit, so they are not taken into account, as well as eventual changes in the auxiliary elements of the powertrain. Considering Eq. (11), the necessity to introduce an iterative process to define the boat weight and performance is clear. M depends upon coefficients that are in turn dependent upon M because of the drag and energy estimates based on the vessel displacement. Therefore, Eq. (11) is placed at the end of the outer loop, which terminates when the absolute difference in estimated mass between successive iterations falls below 1 %. The condition for terminating the outer loop is defined by the following equation:

$$\left|\frac{M_i - M_{i-1}}{M_i}\right| < 1\ \% \rightarrow M = M_i \quad (12)$$

where M_i and M_{i-1} represent the estimated boat mass at the current and previous iterations of the loop, respectively. Once this mass residual condition is satisfied, the boat's parameters are considered fully defined.

3.4. Emissions and costs modelling

Since the power demand and all energy storage related quantities have been computed, it is possible to estimate CO2 emissions and costs. These quantities have been computed on the basis of data collected from a wide variety of research papers, EU Commission reports and National ones, considering the peculiarities of the Egadi scenario. Electricity price and emissions as well as hydrogen ones depend upon the production method and region where they are used. So, to describe the Egadi scenario three main electricity sources and four different hydrogen production methods have been considered. Concerning electricity, the considered sources represent the Italian, the desirable and the current scenarios. The first one is based on the Italian mix of energies to produce electricity and it takes into account the wide range of cost variations related to the user consumption and taxation levels. The other scenarios describe the current Egadi Islands situation, reported in [33], where the almost total dependence on diesel generators for electricity generation is shown, despite the fact that there is far more than enough solar technical energy potential to support the islands' needs. About hydrogen, indeed, the choice to select four different possibilities runs out from their production methods which goes from solar energy (green hydrogen) to natural gas (blue/gray hydrogen) or coal (blue/black hydrogen). As outlined in [54], blue hydrogen can be produced in two ways: the first uses natural gas, while the second uses coal. Blue hydrogen differs from gray hydrogen in that it involves the use of a carbon capture utilisation and storage (CCUS) system starting from natural gas. Similarly, whether hydrogen produced by coal is defined as blue or black depends on the presence or absence of a CCUS system. Please note that black hydrogen is not considered as a possible energy carrier in this paper due to its foul environmental impact. Different sources mean different emissions and costs, which have been accounted for with a specific coefficient for every asset. Greener energy usually means higher costs but zero emissions, while saving on costs means producing more pollutants. Infinite resources would surely lead to the greenest

solution, but a trade off must be met, and so intermediate solutions come into play.

3.4.1. CO_2 emissions

Since this model accounts only for local zero emission powertrains, CO_2 estimates have to be considered placed where the energy production takes place, for example, the location of the electrolyser for the hydrogen production. In other words, emissions from batteries and hydrogen have to be meant as the pollutants emitted during the production of the amount of energy necessary for the specific route and not something that is emitted actually during operations. This approach is similar to an equivalent CO_2 emission estimate but it is only related to the energy consumption and not to all other aspects that contribute to its pure definition. Consumption is caused by the used energy, so by simply integrating the power demand over the time of operations we have the total amount of energy necessary to complete the course. This is a kilo-Watts-per-hour output which allows us to estimate needed electric energy and hydrogen quantity by considering the batteries and FC efficiency. Once these quantities are determined, the corresponding CO_2 emissions are computed as:

$$CO_2 = c_{CO2_B} E_B + c_{CO2_{H2}} E_{H_2} + c_{CO2_D} E_D \tag{13}$$

where c_{CO2_*} are the emission coefficients, provided in Table 5, used to calculate the CO_2 emissions associated with each energy source. Here, E_B, E_{H_2}, and E_D represent the energy supplied by the battery, hydrogen fuel cell, and diesel engine, respectively.

3.4.2. Capital and operational expenditure modelling

Similar to energy consumption, operational and capital costs are functions of the energy used and the power involved. Therefore, they can be estimated in a comparable manner, by simply applying the corresponding cost coefficients, denoted as c_{OP_*} and c_{CA_*}. But, it is needed a distinction between operational expenses/costs (OPEX) and initial capital investment (CAPEX), which has also been made in following analyses. OPEX are to those costs that a company incurs through its normal operations, while CAPEX are funds used by the company to acquire, upgrade, and maintain physical assets such as boats, equipment or other tangible goods. In this paper considered costs are related only to the energy consumption and the boat refitting to greener driveline, in other words, OPEX only takes into account the expenses for energy and CAPEX only considers main expenses for the powertrain substitution, such as engine, battery, fuel cell, electric generator and hydrogen tank costs. Capital investment is not significantly affected by the operations which could only influence the choice between one component or another. On the other hand, operations are the foundation of operative costs, which strongly depend on route, time of operation, displacement and whether conditions which could not be assessed in this paper and require a base of real data to be taken into account. Moreover, OPEX change with the cost of energy necessary to ensure operations which depends strongly on external factors and could fluctuate a lot during time and also change for different regions. The equations used to estimate the operational expenditure (OPEX) and capital expenditure (CAPEX) are given below:

$$OPEX = c_{OP_B} E_B + c_{OP_{H_2}} E_{H_2} + c_{OP_D} E_D \tag{14}$$

$$CAPEX = c_{CA_B} B + c_{CA_{eM}} P_{eM} + c_{CA_{FC}} P_{FC} + c_{CA_{H2}} H_2 \tag{15}$$

the coefficients c_{OP_*} and c_{CA_*}, used to calculate the costs associated with energy use and installed components, are listed in Table 5. Note that Table 5 gives ranges of prices, which could be very large, as in case of green hydrogen, in order to point out results the average of these ranges has been adopted to print out graphs, unless otherwise stated.

4. Analysis and results of the Egadi electrification scenario

This section presents the findings of the parametric model applied to the Egadi scenario. Emissions and costs were calculated considering the specific environmental conditions of this archipelago. The analysis investigated the impact of various boat configurations, including γ, C rating, and energy source production method. To enhance graph clarity, three primary pairs of electricity and hydrogen production methods were selected from a larger set of combinations. These were labeled as Green, Blue, and Gray sources, representing, respectively, the pairing of photovoltaic electricity production and green hydrogen, the Italian energy mix for electricity production and blue or gray hydrogen. Detailed information regarding the fleet and traveled routes can be found in Section 2.1, while all assumed costs and emission coefficients are provided in Section 3.4.

4.1. Analysis of feasible hybrid configurations

The selected route for sizing purposes is *Route S1* (see Section 2.1), which presents the greatest challenge in terms of mileage and energy consumption. As outlined in Section 3.1, various boat configurations were considered, focusing on the balance of hydrogen and battery capacity installed onboard. The energy storage mix naturally influenced the overall boat weight and installed power. Additionally, battery recharge

Table 5
OPEX, CAPEX and CO2 emissions coefficients. Adopted exchange rate 0.90 EUR/USD.

OPEX and CO_2 emissions			
Energy source		OPEX coefficients (c_{OP_i})	CO_2 emissions coefficients (c_{CO2_i})
Diesel [55]		2.081 €/kg (0.176 €/kWh)	2.778 kg_{CO_2}/kg (0.235 kg_{CO_2}/kWh)
Electricity	Italian Scenario [56,57]	0.14288 €/kWh	0.3712 kg_{CO_2}/kWh
	Photovoltaic resources [58]	0.0441 €/kWh	0.0 kg_{CO_2}/kWh
	ICE electric generators[1] [55]	0.4490 €/kWh	0.6894 kgCO2/kWh
Hydrogen [54]	Black (Coal without CCUS)	1.215 €/kg (0.0365 €/kWh)	20 kg_{CO_2}/kg (0.601 kg_{CO_2}/kWh)
	Gray (Natural gas without CCUS)	0.603–1.179 €/kg (0.018–0.035 €/kWh)	8.5 kg_{CO_2}/kg (0.255 kg_{CO_2}/kWh)
	Blue (Coal with CCUS)	1.440–1.845 €/kg (0.043–0.055 €/kWh)	2.4 kg_{CO_2}/kg (0.072 kg_{CO_2}/kWh)
	Blue (Natural gas with CCUS)	0.891–1.647 €/kg (0.027–0.049 €/kWh)	1.0 kg_{CO_2}/kg (0.030 kg_{CO_2}/kWh)
	Green (Renewable sources)	2.016–7.056 €/kg (0.060–0.212 €/kWh)	0.0 kg_{CO_2}/kg (0.00 kg_{CO_2}/kWh)
CAPEX			
Component		CAPEX coefficients (c_{CA_i})	
Battery [59]		308 €/kWh	
Electric motor [20]		124.20 €/kW	
PEM Fuel Cell [20]		920 €/kW	
Hydrogen tank [60]		500 €/kgH_2 (15.01 €/kWh)	

[1] Cost of electricity production by means of ICE generators has been computed based on the assumption of an SFC equal to 0.2 kg/kWh.

performance, which significantly impacts the installed battery capacity, was taken into account through the C rating, which ranged from 0.2 to 1 to highlight the associated trend. To avoid excessively large battery packs that might not be feasible in a retrofitting project, an arbitrary and representative constraint was imposed, limiting battery weight to less than 25 % of the overall boat weight. Fig. 15 summarizes the key boat characteristics, including required energy, installed energy, motor power, and boat weight, as functions of γ at different C ratings. Dashed gray lines indicate unconsidered configurations where the battery weight exceeded the 25 % limit. These quantities exhibit similar trends due to their strong interconnections, providing valuable insights. Primarily, full hydrogen solutions ($\gamma \rightarrow 1$) require less component weight, resulting in lower power and required energy. However, they might necessitate more onboard capacity compared to high C rating, lower γ configurations because of the lower efficiency of FC in converting hydrogen to electricity compared to a battery storage. Another notable trend is the significant impact of C rating on all curves, demonstrating a strong dependency that leads to a reduction in required battery pack capacity (when C increases), affecting weight and other factors. It's essential to note that if battery recharging during operations is not permitted, this trend may not accurately reflect the real scenario. In such a case, the entire route's required energy would need to be stored in the battery pack and hydrogen tanks from the initial departure, leading to a significantly higher demand. Indeed, the estimated energy requirement for a vessel that cannot recharge during operation has been calculated to be approximately 55 MWh for a full battery configuration and nearly 25 MWh for a full hydrogen configuration, which are considered as unfeasible solutions. The trends presented in Fig. 15 are not solely driven by the factors discussed but are also subject to the individual efficiencies of the FCs and batteries. This dependency is further elaborated in Fig. 16, which demonstrates how varying efficiencies (up to ±5.0 %) establish boundaries for the observed trends. The required energy reported in Fig. 15 represents the total energy needed to complete the entire route, which differs from the installed energy due to battery discharge and fuel cell efficiencies. The disparity between these efficiencies distorts the installed energy curves compared to the required energy ones, amplifying the impact of C rating on boat characteristics. Fig. 17 illustrates the breakdown of installed energy, separately showing battery capacity and hydrogen capacity. As γ increases, hydrogen capacity also rises, but notable variations emerge due to C rating. Curves with C values below 0.5 exhibit a clear maximum that shifts toward higher γ values as C increases. Conversely, battery capacity trends closely resemble those of boat weight and installed power, clearly demonstrating the imposed battery size constraint, as evidenced by the distinct division between the dashed gray lines and the colored ones. These trends directly influence costs and CO_2 emissions, which can be estimated as described in Section 3.4.

4.2. Blending factors impact on capital expenditure

Fig. 18 presents the parametric model outcomes on CAPEX. Significant variations in terms of millions of euros are observed in the estimated costs of acquiring the components for each boat configuration. As anticipated, higher hydrogen capacity generally leads to higher CAPEX. However, this is not entirely accurate. The blue curve, representing a very low battery C rating, exhibits a minimum point, indicating a trade-off between large battery packs and the high costs of fuel cells. Battery packs significantly impact CAPEX due to their substantial size and high cost per kWh. Consequently, the C rating, which affects battery pack size, plays a crucial role in estimating capital investment. It's important to note that these estimates only account for the cost of individual components and do not include installation costs or necessary secondary components. Additionally, the battery price does not currently factor in C rating (due to a lack of available references), but it is reasonable to expect that higher C ratings would increase battery prices. This effect could potentially narrow the gap between CAPEX curves, benefiting low C configurations.

4.3. Operational expenditure and emissions

The initial high cost to acquire new components can be economically justified by saving on operative costs. Indeed OPEX are much lower than estimated operative cost of the initial boat configuration. This is mainly due to the huge difference in efficiency of an electric boat compared to an ICE propelled one, moreover electricity costs less than diesel, contributing to maintaining a cost reduction even with an increase in required energy (configurations with lower γ). Fig. 19a compares trends of energy production methods pairs described in Section 4 for a fixed C rating (C_{ref} equal to 0.6). Some interesting information can be derived from this graph: Blue and Gray sources exhibit a quite similar trend, dropping their cost for higher hydrogen capacity installed onboard, with a marked distinction between the two lines only after $\gamma \sim 0.6$, on the other hand, Green sources increase their cost with γ because of the really high price of green hydrogen, which despite the lower energy demand increase operative costs. Note that costs for hydrogen have been considered equal to the mean value of ranges reported in Table 5.

Fig. 19b reports the cost reduction against the original boat configuration. This quantity has been computed as:

$$OPEX_{red}(\gamma) = \frac{OPEX(\gamma, C = C_{ref}) - OPEX_{Admiral\,250}}{OPEX_{Admiral\,250}} \tag{16}$$

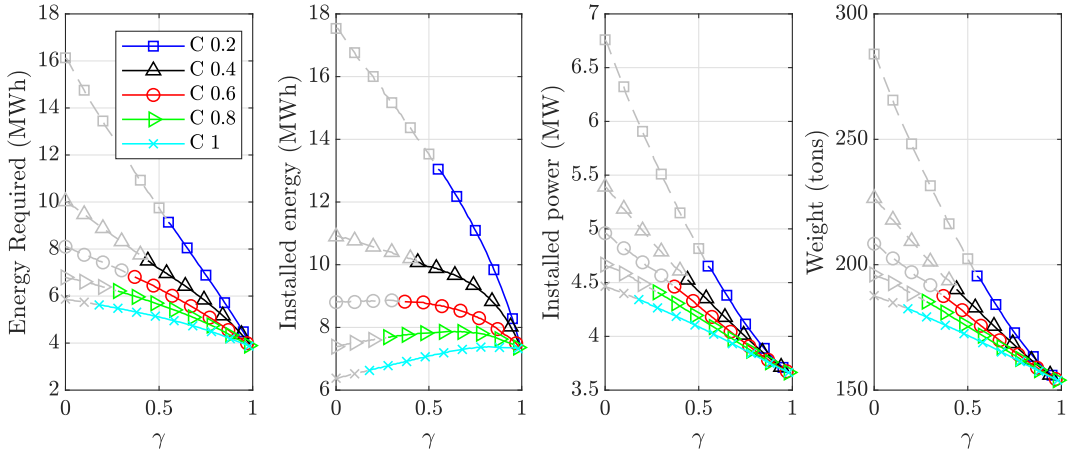

Fig. 15. Energy required, installed power and overall weight trends by changing γ and C rating.

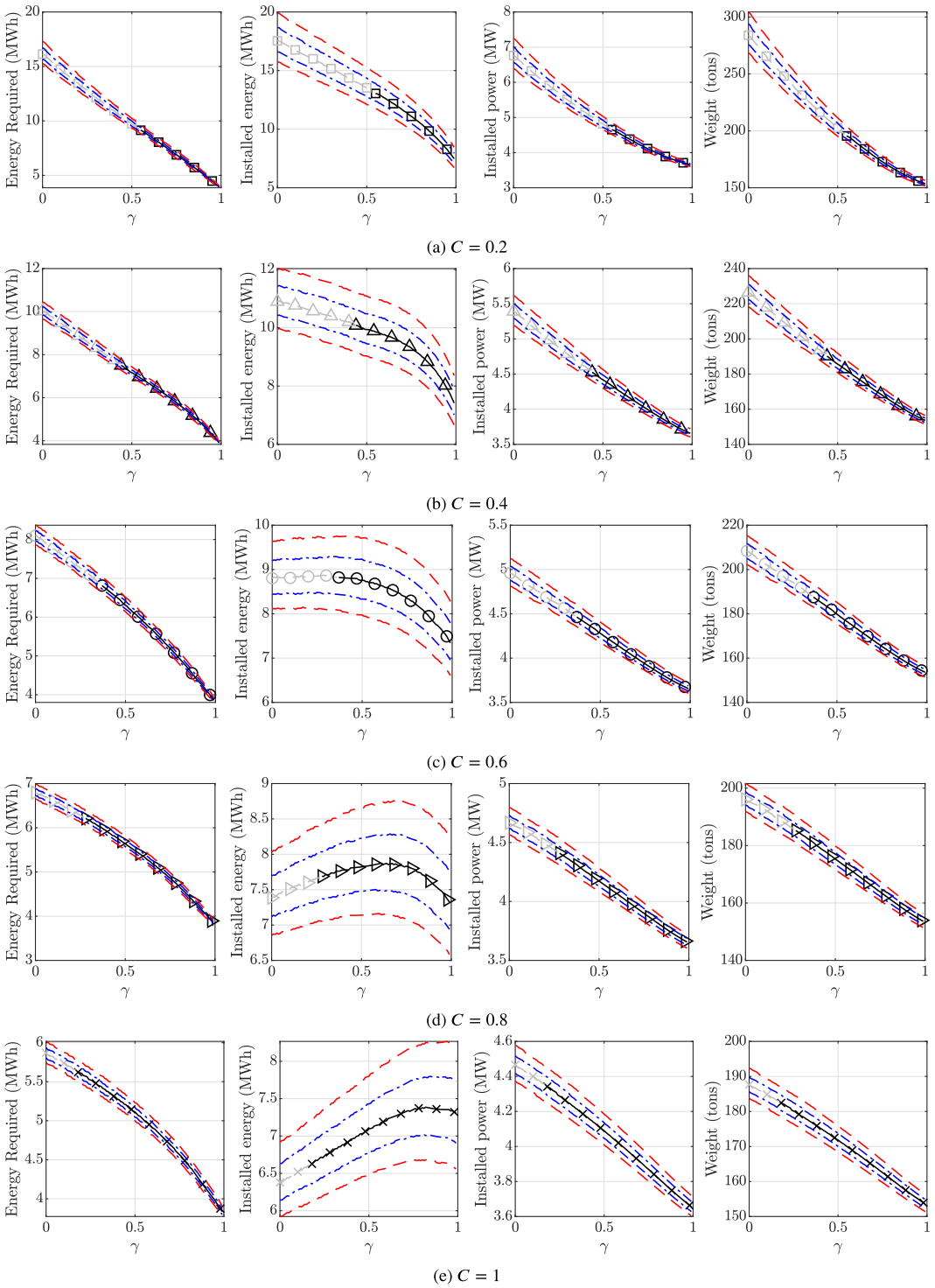

Fig. 16. Sensitivity of required energy, installed power, and overall weight to variations in fuel cell (FC) and battery efficiencies. The blue and red dashed curves illustrate trends corresponding to efficiency variations of ±2.5 % and ±5.0 %, respectively.

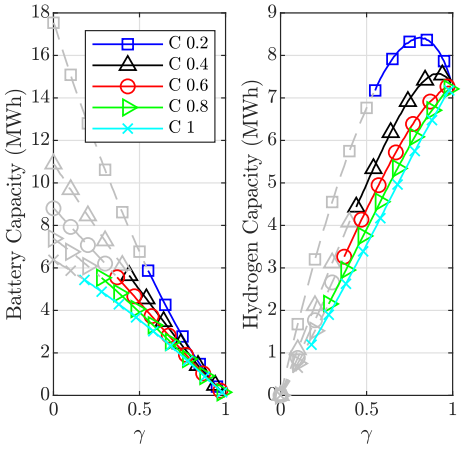

Fig. 17. Energy storage composition variation with γ.

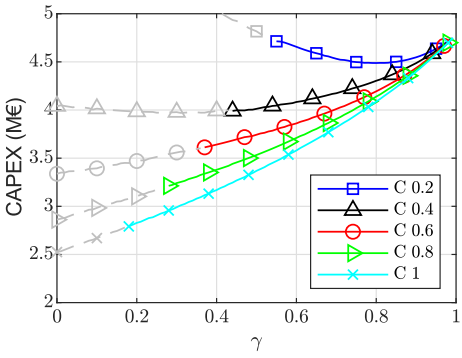

Fig. 18. CAPEX trend by changing γ and C rating.

When considering high values of γ, Blue and Gray sources are anticipated to exhibit a reduction of over 80 %. In contrast, Green sources are expected to experience a similar OPEX reduction at low values of γ. In Fig. 19, both plots feature a shaded area for every energy source pair. These shaded regions illustrate the potential range of OPEX and OPEX reduction values, considering price fluctuations on the order of ±20 %. The same figure shows trends for a fixed C but this parameter affects the boat characteristics and so operative costs. In order to point out the effect of C on OPEX, the variation of this quantity has been computed with respect to the trends reported in Fig. 19a as follows:

$$\Delta OPEX(\gamma) = OPEX(\gamma, C) - OPEX(\gamma, C = C_{ref}) \tag{17}$$

Results of this computation have been reported in Fig. 20, where the OPEX sensitivity to the C rating is pointed out for the three depicted energy source pairs. It is noticeable the large variation for the Green Sources at low C ratings, which is linked to the higher price of green hydrogen and the higher amount of energy required in that region against to the one depicted in Fig. 19a. Blue and Gray sources display similar trends which marks a larger variation for lower values of γ, which is also the region where the effect of C rating variation is higher.

Even though, the economic aspects are relevant, the most significant achievement of a fleet electrification is the environmental impact reduction. CO_2 emissions have been computed for the Egadi scenario as reported in Section 3.4.1, referencing to energy production method pairs described in Section 4 and a fixed C rating (the same adopted in Section 4.3). Fig. 22 shows the outcomes of these estimates. It reports the CO_2 emissions (in tons) as a function of γ and the percentage reduction compared to the reference boat (6.82 tons per day on *Route S1*), which has been computed as:

$$CO_{2_{red}}(\gamma) = \frac{CO_2(\gamma, C = C_{ref}) - CO_{2_{Admiral\ 250}}}{CO_{2_{Admiral\ 250}}} \tag{18}$$

Green, Blue and Gray sources solutions outcomes are quite different and their environmental impact is deeply dissimilar: Green sources doesn't provide any pollutant in all boat configurations so they reduce of 100 % the original CO_2 boat emissions, while Blue ones, ensure for all γ a CO_2 emission level lower than the original boat, starting from an almost 15 % to 90 % of expected CO_2 reduction while γ increases. On the other hand, Gray sources, maintain a quite stable level of CO_2 emissions with γ but the induced reduction is the lowest achievable and moreover, comparable to the original boat emission (less than 15 % of reduction). These statements underline how the way in which electrification is conducted change the environmental benefit because of the way electricity and other involved energy vectors (in this case hydrogen) are produced. Note that the environmental impact due to poor production methods has to be meant in production area and not in the Egadi Archipelago, so in a local point of view the electrification will totally cut the CO_2 emissions related to the passenger transportation. As done for the OPEX, a sensitivity analysis has been conducted on the C rating effect on the CO_2 emissions. The CO_2 variation has been computed as:

$$\Delta CO_2(\gamma) = CO_2(\gamma, C) - CO_2(\gamma, C = C_{ref}) \tag{19}$$

and its results have been reported in Fig. 21, where the differences between Blue and Gray sources are substantial even if the regions of

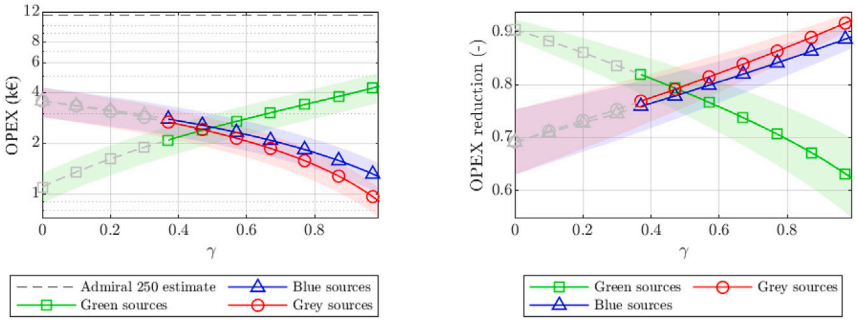

(a) OPEX variation

(b) OPEX reduction

Fig. 19. OPEX variation with γ.

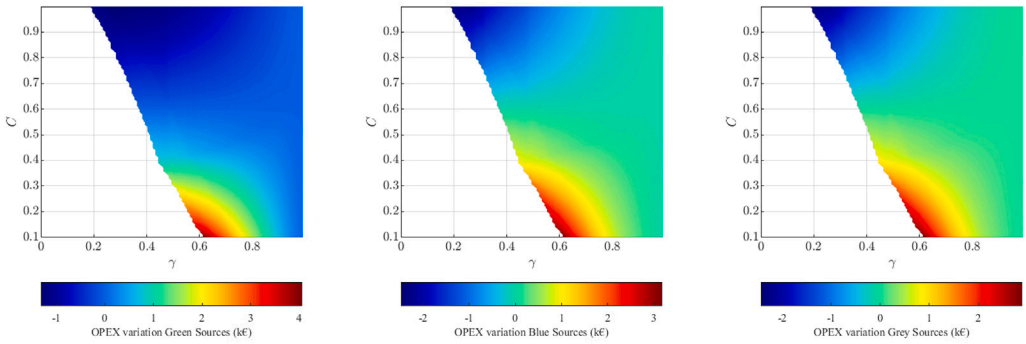

(a) Green solution (b) Blue solution (c) Gray solution

Fig. 20. OPEX sensitivity to γ and C rating.

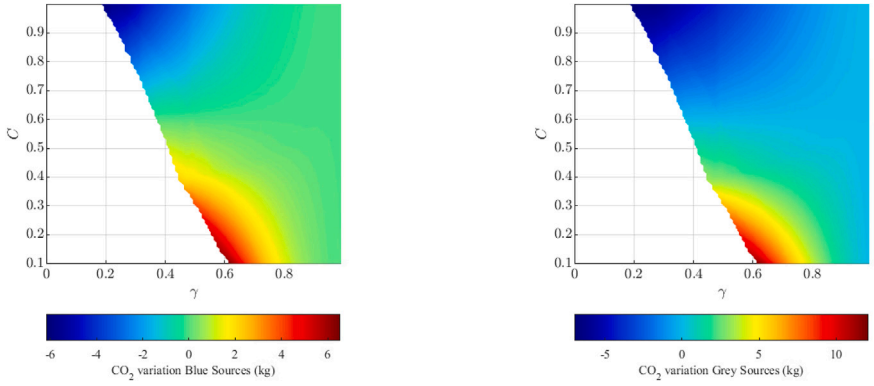

(a) Blue solution (b) Gray solution

Fig. 21. CO2 sensitivity to γ and C rating.

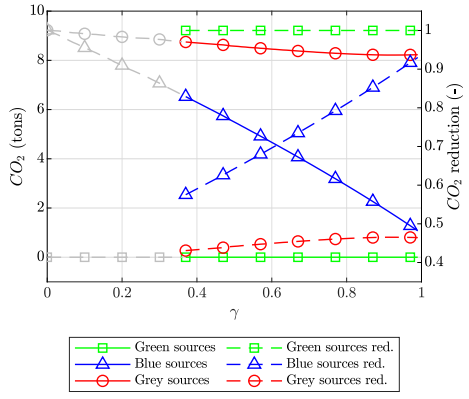

Fig. 22. CO2 emission.

increase and decrease of the expected emissions are quite similar. The sensitivity analysis for the Green sources has not been reported simply because it does not produce any variation with the C rating, it always emits 0 kg CO_2 into the atmosphere. The reduction of emissions is frequently subordinated to the pursuit of enhanced economic benefits. To illustrate this point, the operating costs and emissions have been plotted on the same graph at varying γ for the three energy scenarios thus far considered, Fig. 23. Each potential energy solution brings with it a trend that is markedly distinct from the others, exhibiting the following characteristics. In the case of energy production from fully renewable sources (Green sources), emissions would remain constant (0 kg CO_2) and OPEX would increase in proportion to the fraction of hydrogen considered in the design of the boat. Conversely, the most polluting solution (Gray sources) demonstrates a considerable range in cost, while maintaining emissions at a consistently elevated level in comparison to the other solutions. The intermediate scenario (Blue sources) is of particular interest due to its distinctive characteristics. It displays a notable degree of variability in costs, coupled with a similar degree of variability in emissions, allowing the attainment of low emission and cost values. Both non-renewable solutions offer financial incentives for the use of hydrogen in place of electric batteries. Conversely, the cost increase associated with the fraction of hydrogen installed on board, in the Green sources solution, can be attributed solely to the high cost of green hydrogen.

5. Long-term economic and emission projections

The presented results are based on simulations for a single vessel operating on a single route over the course of one day. However, they can also be extrapolated to provide a preliminary long-term estimate of the overall expenditure for the entire fleet. To this end, a preliminary assessment has been conducted to estimate the time required for the operational expenditure savings relative to the original vessel configuration to offset the capital expenditure investment. This duration, referred to as the payback time (PT), provides an initial indication of

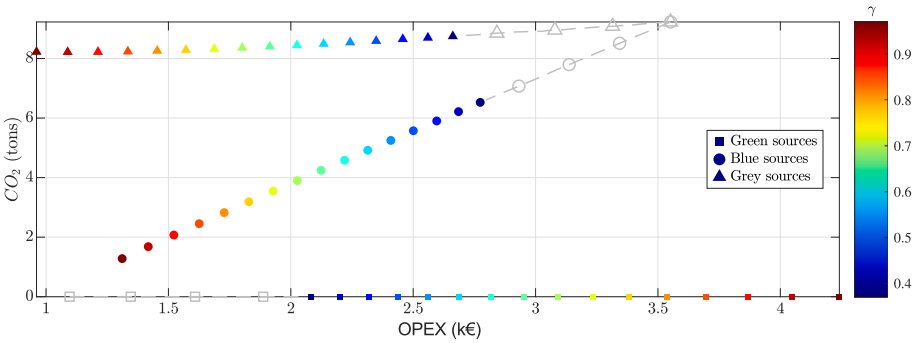

Fig. 23. CO2 emission function of OPEX and γ.

the economic feasibility of the proposed configuration. This estimate has been made referencing to outcomes of the considered route, so they will change with route characteristics and required performances, due to the different energy requirement and so operative costs and emissions. Fig. 24 summarize these outcomes with same conditions used for Fig. 19a.

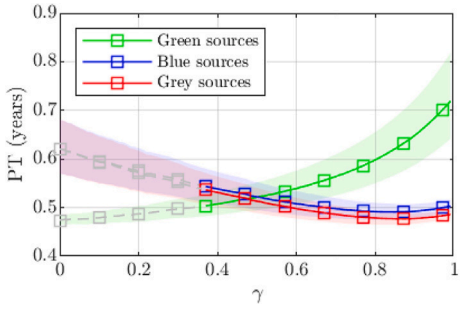

Fig. 24. Time for OPEX reduction induced savings to equalize CAPEX investment (Payback Time).

Blue and Gray sources lead to a quite stable PT which is almost half a year and doesn't change a lot with γ, even if a small reduction is visible. On the other hand, Green sources lead to solution whose PT change a lot with γ, almost doubling the PT from the lowest to the highest admitted value of γ. As made for Fig. 19, the shaded areas in the plot represent the PT variations due to an OPEX variation in the range of ± 20 %. Make it clear that these estimates have been made on the computed OPEX and CAPEX, which accounts only for a portion of the real costs, so this PT parameter could be better explained as the time required by savings on energy purchase to equalize the capital investment required to buy retrofit components.

Based on these findings, a hypothetical retrofit plan has been developed extending through 2050. This plan assumes the replacement of one vessel every three years, an interval longer than all projected payback times (PT), to ensure a timely return on investment. The proposed accelerated replacement schedule is designed to achieve a fully upgraded fleet of five operational vessels, capable of servicing all planned routes within a 15 year horizon. To explore long-term performance and economic trends, three different vessel configurations were analyzed, corresponding to γ values of 0.45, 0.75, and 0.99, each evaluated with a fixed C rating of 0.6. The resulting trends are illustrated in Fig. 26. Fig. 26a illustrates the diverse potential scenarios for the fleet up to 2050, ranging from complete decarbonization to a scenario that cuts pollutants by half compared to the original fleet. Notably, the use of gray sources can lead to CO_2 emissions that could be considered in line with the IMO expectations [3]. Considering Blue sources, interestingly, the solution resulting in a larger reduction of CO_2 emissions is the one with the largest share of hydrogen (high value of γ). This high reduction compared to the results for the same sources, but with a γ of 0.45, is the result of a significant reduction in energy requirements and a reduced installed power thanks to the weight savings. Moreover it is noticeable how Blue sources solutions are perfectly bounded by Green and Gray ones. Green sources lead to a total decarbonization in 15 years but there are also Blue sources configurations that lead to a very desirable scenario. In conjunction with the CO_2 emission forecast, operational expenses (OPEX) were projected up to 2050. Fig. 26b illustrates the diverse range of anticipated expenses that the company could incur due to the selection of different energy sources and their blending. Despite the CO_2 forecast, OPEX results aren't so well bounded between two different energy source pairs. Indeed, Green and Gray sources are placed at extremes, but some of their configurations are in the middle of the OPEX forecast range. These OPEX estimates are based on today's price estimates, but they will change. Some trends are available for the expected price trends of green sources, particularly PV and green hydrogen. This means that these trends can be updated with the expected prices for them over time. Fig. 26c shows these results, comparing projections obtained using current prices (Scenario 0, $S.0$) with projections considering green hydrogen prices for the EU region according to Source [62] (average condition, AC) and PV according to [61] (Scenario 1, $S.1$), and then projections considering green hydrogen prices for the Italian region according to [63] and PV according to [61] (Scenario 2, $S.1$). These price projections are reported in Fig. 25b and demonstrate the high uncertainty of green hydrogen price projections, as depicted by the shaded area (the range between the optimal condition, OC, and the unfavourable one, UC). Furthermore, Fig. 25b shows that the medium-term expectations for the Italian region according to [63] are much higher than those expected for the entire EU area. On the other hand, PV projections show a significant reduction in electricity prices, albeit lower than that of green hydrogen. The data used to create Fig. 25b are also available in Table 6. It is notable that the projections from Scenarios 1 and 2 are delayed due to significant differences in the expected prices for the two references. Unfortunately, data like this is unavailable for the blue and gray sources, so Fig. 26c only shows the OPEX trend comparison for the green sources. It's important to note that while fixing the C rating of the batteries in these plots does influence the proposed trends, this impact is relatively minor compared to the effect of the γ value. Fig. 27 presents a cumulative representation of the data depicted in Fig. 26. It highlights the substantial environmental benefits associated with reduced CO_2 emissions, which can also lead to savings in operational costs. Fig. 27b illustrates the capital expenditures (CAPEX) over the entire timeframe, which constitute a relatively small portion of the operational costs for all considered configurations. Following the same approach as in Fig. 25a, trends in prices for batteries and fuel cells (FCs) are available up to 2050. Fig. 27c shows the variation in CAPEX estimates when considering or not considering the price variation of FCs and batteries (reported as $CAPEX^*$ and $CAPEX$, respectively). As shown in Fig. 25a, which depicts data from Ref. [62] and [61] for

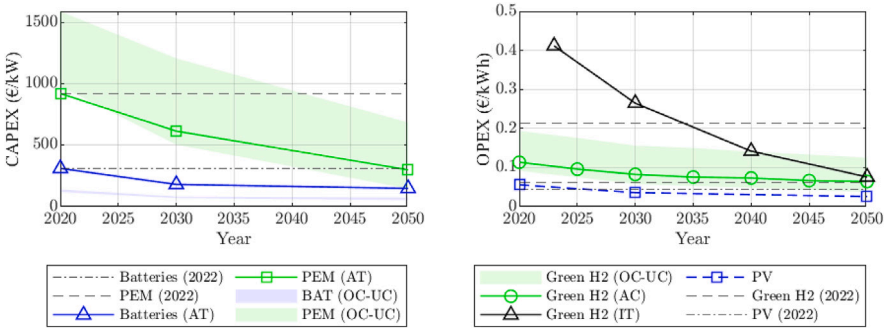

(a) PEM and Batteiries price projections up to 2050

(b) Green H_2 and PV price projections up to 2050

Fig. 25. Projections of prices up to 2050.

PEM and batteries respectively, the prices of both systems will decline. As for green hydrogen prices, PEM FCs show high uncertainty, as indicated by the shaded area (between optimal, OC, and unfavourable, UC, conditions). Note that, since a significant discrepancy is reported between Sources [61] and [59] regarding the price of batteries (which is expected to be explained by different accounting methods for systems that define a battery, such as just the cells or the cells and the systems required to control the battery), it was decided to use values from Source [59], which refers to a specific naval application and also represents a higher estimate, and then apply the percentage reduction suggested by Source [61]. These data are also reported in Table 6. Since the expected cost reductions are significant, the trends depicted in Fig. 27c show a substantial cumulative CAPEX reduction over time. As previously mentioned, these trends only consider the costs of components (CAPEX) and hydrogen/electricity consumption (OPEX). Therefore, they represent a portion of the total expenditure, albeit likely the most significant one. While the most environmentally beneficial option may not always coincide with the most financially advantageous one, there are numerous scenarios that offer a favourable balance between economic and environmental factors.

5.1. Electrification feasibility, infrastructure, and broader benefits

Based on the findings of this case study, fleet electrification appears to be a viable option. However, there are several additional factors beyond the scope of this study, including the infrastructure required to support the entire fleet and the practical feasibility of retrofitting existing boats compared to purchasing new electric vessels. While the second argument involves considerations that extend beyond data-driven analysis and are influenced by company-specific decisions, the potential

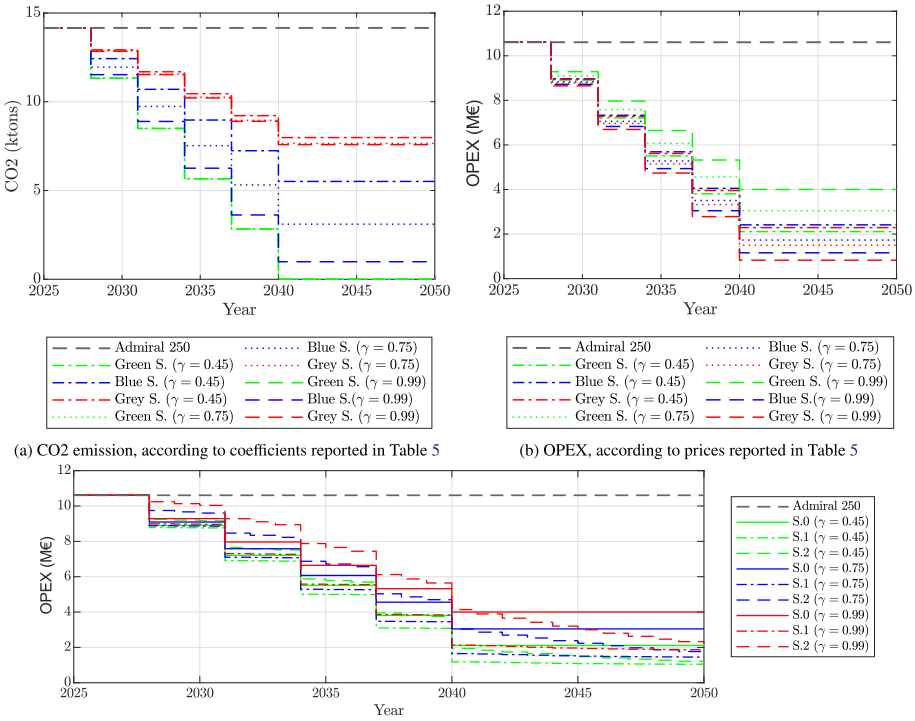

(a) CO2 emission, according to coefficients reported in Table 5

(b) OPEX, according to prices reported in Table 5

(c) Green sources scenario OPEX for different cost projections (see Figure 25b). Scenario 0 (*S*.0), no prices update; Scenario 1 (*S*.1), green sources prices according to EU projections; Scenario 2 (*S*.2), green sources prices according to Italian projections;

Fig. 26. Retrofit plan, up to 2050, yearly based estimate.

Table 6
OPEX and CAPEX price projections up to 2050.

		Year		
		2020	2030	2050
CAPEX	Batteries [61]	115.7–137.95 €/kW	66.75–80.1 €/kW	48.95–71.2 €/kW
	PEM [62]	976.43–1590.46 €/kW	502.47–1206.51 €/kW	143.12–683.27 €/kW
OPEX	PV [61]	0.055 €/kWh	0.035 €/kWh	0.025 €/kWh
	Green H_2 [62]	0.091–0.193 €/kWh	0.057–0.155 €/kWh	0.036–0.124 €/kWh
	Green H_2 (IT) [63]	0.411 €/kWh (2023)	0.264 €/kWh	0.075 €/kWh

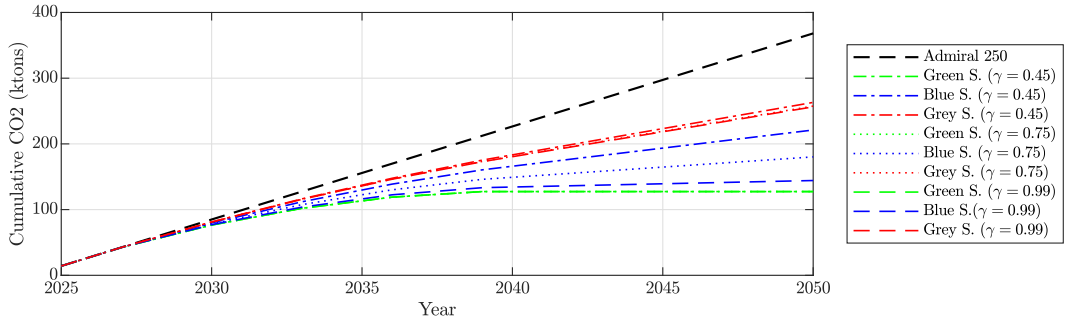

(a) CO2 emission, according to coefficients reported in Table 5

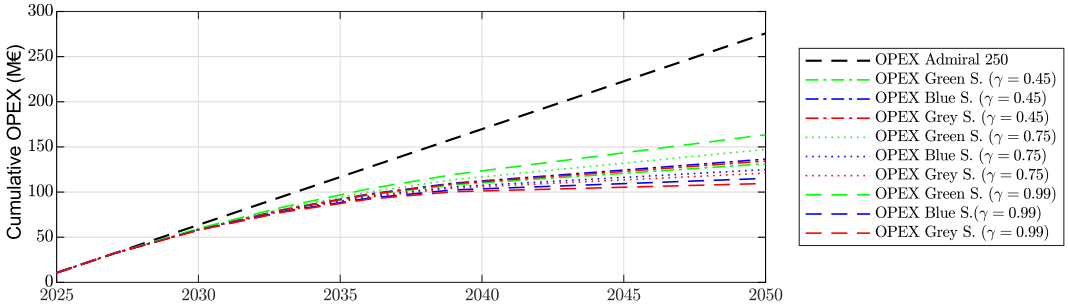

(b) OPEX, according to prices reported in Table 5

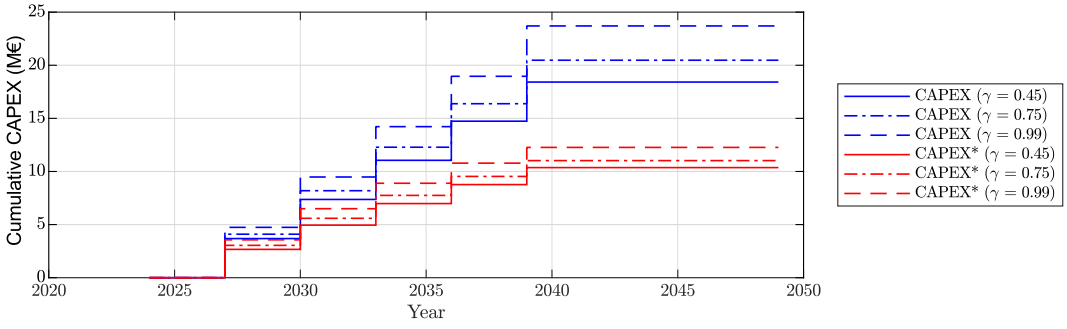

(c) CAPEX projections, with ($CAPEX^*$) and without ($CAPEX$) Batteries and PEM cost projections (see Figure 25a)

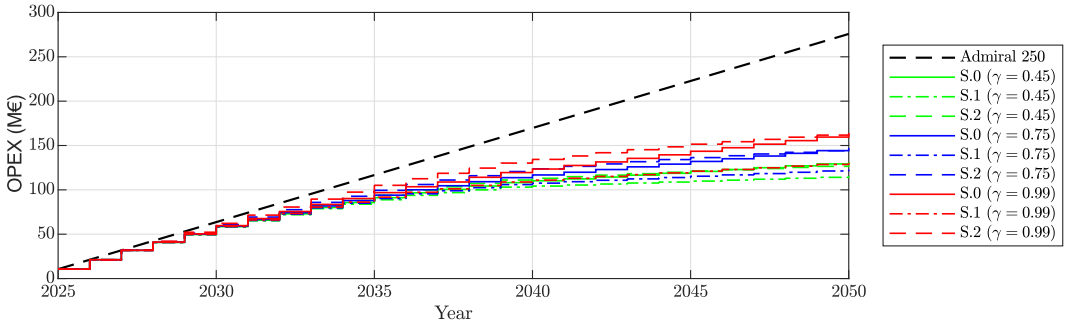

(d) Green sources scenario OPEX for different cost projections (see Figure 25b). Scenario 0 ($S.0$), no prices update; Scenario 1 ($S.1$), green sources prices according to EU projections; Scenario 2 ($S.2$), green sources prices according to Italian projections;

Fig. 27. Retrofit plan, up to 2050, cumulative projection.

impacts of infrastructure can be factored into even this preliminary stage of the work. It's important to note that all calculations presented in this study assume that boats recharge only in Trapani and Marsala, both of which are on the Sicilian mainland and connected to the Italian electrical grid. However, a potential alternative scenario involves the Egadi Archipelago generating sufficient electricity to power its own fleet, enabling recharging even on smaller islands [33,64]. According to data from ESCAPE [33], the Egadi Archipelago possesses a significantly higher photovoltaic technical potential than its current energy consumption (latest data update 2019), suggesting that there is a potential margin for powering an electric fleet (refer to Fig. 28). It's important to note that [33] data is preliminary, and the estimated potential energy production may be overstated. Additionally, while these lines focus on photovoltaic sources, Moscoloni et al. [33] also report on other renewable energy sources in the region, such as wind, geothermal, and wave power, which further increase the available green energy. Introducing green energy sources in the Egadi Archipelago, where electricity is primarily generated by diesel generators [33], would not only benefit the environment but also improve the quality of life for the local population. This scenario could pave the way for boats with significantly lower energy consumption, potentially leading to reduced weight, decreased power requirements, and further reductions in operational costs and initial capital investment. Additionally, the potential to introduce boats with smaller installed capacity could lead to a reassessment of the entire fleet, focusing on smaller vessels that can increase connectivity throughout the year, both during summer and winter months. This would enable better route planning and further enhance economic and environmental benefits.

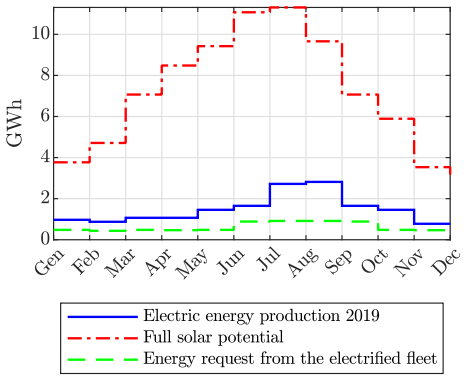

Fig. 28. Comparison between the full solar potential of the Egadi archipelago, its energy demand (in 2019) and the estimated energy request of the electrified fleet.

6. Conclusion

The mobility scenario on small islands like those in the Egadi Archipelago necessitates a careful balance between meeting transportation needs and protecting the environment. By embracing electric propulsion, integrating renewable energy sources, implementing supportive policies, and fostering public awareness, small islands can develop sustainable mobility systems that enhance quality of life, support tourism, and safeguard their unique ecosystems. This overview underscores the importance of a holistic approach to mobility that considers both technological advancements and community engagement in achieving sustainable development. The methodology described in this work enables the generation of qualitative estimates for the electrification of an entire fleet using a limited set of readily available input data. It holds strong potential for application and adaptation across a wide range of operational scenarios. It is important to emphasize that a study of this nature necessarily relies on a series of assumptions and simplifications, which are essential for deriving hydrofoil design parameters from minimal inputs such as vessel speed and mass. Although the results are qualitative, they can serve as an initial, exploratory step in the planning process for fleet-wide or single-vessel retrofitting. The methodology facilitates rapid screening of multiple hybrid configurations and provides insights into the potential trade-offs between different energy vectors in terms of costs and emissions.

According to the model results, introducing an electrified fleet in the archipelago would yield a substantial reduction in pollutant emissions (Fig. 26a): up to 46 % compared to current CO_2 levels when using gray energy sources, and up to 91 % when adopting greener (blue) alternatives. Additionally, depending on the vessel configuration, the operational costs (OPEX) of a fleet powered by green energy sources are projected to decrease by 62–85 % relative to current costs by 2050, the year in which, under the proposed retrofit plan, all vessels are expected to be equipped with electric propulsion (Fig. 26c). Furthermore, the capital investment required for the transition is projected to be recouped in a relatively short period, primarily due to OPEX savings (Fig. 24). Specifically, the payback time is estimated to average 0.47 years for a fully hydrogen-powered configuration using gray sources, and up to 0.82 years when using green sources. These figures are expected to decline further in the coming years as the costs of batteries, FC systems, and renewable energy sources decrease (Fig. 25). For battery-dominant configurations, the influence of the energy source on the payback time is reduced, with average values around 0.53 years for $\gamma = 0.4$, based on current cost estimates for FCs and battery storage.

Future developments of the model may include improvements in the prediction of power demand along the route, integration of additional parameters to handle more complex operating scenarios, and consideration of mixed vessel types within the fleet. Eventually, the scope could be expanded to include optimization of the fleet size itself, allowing for variable numbers of vessels that are tailored to service the planned routes efficiently through schedule and energy-use optimization. Moreover, incorporating detailed information on available inland infrastructure for recharging and refueling—both on the mainland and on the islands—will enhance the accuracy of predictions and support the identification of feasible and regionally appropriate solutions. This refinement could result in lower energy requirements for each route, enabling lighter, less costly, and more efficient vessel configurations.

An electrified fleet would not only drastically reduce CO_2 emissions, but also offer a sustainable economic model for stakeholders, particularly when paired with long-term planning strategies. The potential to generate sufficient photovoltaic energy on the islands to meet the fleet's total energy demand makes this scenario even more appealing, offering the possibility of a zero-emission, self-sustaining maritime network. Such a transformation would provide significant benefits to the local population, both economically and in terms of public health.

CRediT authorship contribution statement

Francesco Balestrieri: Writing – review & editing, Writing – original draft, Visualization, Software, Methodology, Investigation, Data curation, Conceptualization. **Alessandro Brusasco:** Writing – review & editing, Visualization, Software. **Matteo Melchiorre:** Writing – review & editing, Supervision, Conceptualization. **Mauro Bonfanti:** Writing – review & editing, Writing – original draft, Supervision, Methodology, Formal analysis, Conceptualization. **Stefano Mauro:** Writing – review & editing, Supervision, Project administration, Funding acquisition, Conceptualization.

Declaration of generative AI and AI-assisted technologies in the writing process

During the preparation of this work, the authors used the AI-based language model Gemini by Google, in order to improve the spelling, language, and grammar of this paper. After using these tools/services, the authors reviewed and edited the content as needed and take full responsibility for the content of the publication.

Declaration of competing interest

The authors declare that they have no known competing financial interests or personal relationships that could have appeared to influence the work reported in this paper.

Acknowledgments

This publication is part of the project PNRR-NGEU which has received funding from the MUR–DM117/2023 and the MUR-DM630/2024. It is also part of the project NODES which has received funding from the MUR – M4C2 1.5 of PNRR with grant agreement no. ECS00000036.

Data availability

Data will be made available upon request.

References

[1] Marine Environmental Protection Committee. Amendments to the annex of the protocol of 1997 to amend the international convention for the prevention of pollution from ship, 1973, as modified by the protocol of 1978 relating thereto. 2011 15 July;203(62).
[2] Tadros M, Ventura M, Soares CG. Review of current regulations, available technologies, and future trends in the green shipping industry. Ocean Eng 2023.
[3] Marine Environmental Protection Committee. Initial IMO strategy on reduction of GHG emissions from ships 2003 13 April;304(72).
[4] Feng R, Hua Z, Yu J, Zhao Z, Dan Y, Zhai H, et al. A comparative investigation on the energy flow of pure battery electric vehicle under different driving conditions. Appl Therm Eng 2025.
[5] NASA. Global climate change; 2023.
[6] Ampah JD, Yusuf AA, Afrane S, Jin C, Liu H. Reviewing two decades of cleaner alternative marine fuels: towards imo's decarbonization of the maritime transport sector. J Clean Prod 2021.
[7] Rufer C. Ammonia - fuel for net-zero. Technical report, MAN Energy Solutions; 2024.
[8] Renter K, Gruschwitz F. Energy transition with hydrogen. Technical report, MAN Energy Solutions; 2022.
[9] Vogtle U. Decarbonise now with lng-to-power. Technical report, MAN Energy Solutions; 2021.
[10] Moradi MH, Brutsche M, Wenig M, Wagner U, Koch T. Marine route optimization using reinforcement learning approach to reduce fuel consumption and consequently minimize co2 emissions. Ocean Eng 2022.
[11] Lv Z, Lv H, Fridenfalk M. Digital twins in the marine industry. Electronics 2023.
[12] Ahlgren F, Thern M. Auto machine learning for predicting ship fuel consumption. In: Proc ECOS 2018 31st Int Conf Eff Cost Optim Simul Environ Impact Energy Syst Guimarães, 2018.
[13] Zha L, Zhu R, Hong L, Huang S. Hull form optimization for reduced calm-water resistance and improved vertical motion performance in irregular head waves. Ocean Eng 2021.
[14] Yang S, Yuan J, Nian V, Li L, Li H. Economics of marinised offshore charging stations for electrifying the maritime sector. Appl Energy 2022.
[15] Artemis Technologies. Welcome to our world: leading the decarbonisation of the maritime industry; 2025.
[16] Ajanovic A, Sayer M, Haas R. On the future relevance of green hydrogen in europe. Appl Energy 2024.
[17] Béres R, Nijs W, Boldrini A, van den Broek M. Will hydrogen and synthetic fuels energize our future? Their role in Europe's climate-neutral energy system and power system dynamics. Appl Energy 2024.
[18] Mallouppas G, Yfantis EA. Decarbonization in shipping industry: a review of research, technology development, and innovation proposals. J Mar Sci Eng 2021;9.
[19] Elkafas AG, Rivarolo M, Gadducci E, Magistri L, Massardo AF. Fuel cell systems for maritime: a review of research development, commercial products, applications, and perspectives. Processes 2023.
[20] Fu Z, Lu L, Zhang C, Xu Q, Zhang X, Gao Z, et al. Fuel cell and hydrogen in maritime application: a review on aspects of technology, cost and regulations. Sustain Energy Technol Assess 2023.
[21] Sürer MG, Arat HT. Advancements and current technologies on hydrogen fuel cell applications for marine vehicles. Int J Hydrogen Energy 2022;47.
[22] Korkmaz SA, Erginer KE, Yuksel O, Konur O, Colpan CO. Environmental and economic analyses of fuel cell and battery-based hybrid systems utilized as auxiliary power units on a chemical tanker vessel. Int J Hydrogen Energy 2023.
[23] Sundvor I, Thorne RJ, Danebergs J, Aarskog F, Weber C. Estimating the replacement potential of Norwegian high-speed passenger vessels with zero-emission solutions. Processes 2023.
[24] Miretti F, Misul D, Gennaro G, Ferrari A. Hybridizing waterborne transport: modeling and simulation of low emissions hybrid waterbuses for the city of venice. Energy 2022.
[25] Mojarrad M, Thorne RJ, Rodseth KL. Technical and cost analysis of zero-emission high-speed ferries: retrofitting from diesel to green hydrogen. Heliyon 2024.
[26] Wang H, Boulougouris E, Theotokatos G, Zhou P, Priftis A, Shi G. Life cycle analysis and cost assessment of a battery powered ferry. Ocean Eng 2021.
[27] Papanikolaou A, Xing-Kaeding Y, Strobel J, Kanellopoulou A, Zaraphonitis G, Tolo E. Numerical and experimental optimizatio study on a fast, zero emission catamaran. J Mar Sci Eng 2020.
[28] Chiche A, Andruetto C, Lagergren C, Lindbergh G, Stenius I, Peretti L. Feasibility and impact of a Swedish fuel cell-powered rescue boat. Ocean Eng 2021.
[29] Rodseth KL, Fagerholt K, Proost S. Optimal planning of an urban ferry service operated with zero emission technology. Marit Transp Res 2023.
[30] Michel WH, Hoerner SF, Ward LW, Buermann TM. Hydrofoil handbook. Technical report, Naval Research Navy Department; 2023.
[31] Buermann TM, Leehey P, StilWell JJ. An appraisal of hydrofoil supported craft. Proc Soc Nav Archit Mar Eng 1953.
[32] D'Anna G, Fernández TV, Pipitone C, Garofalo G, Badalamenti F. Governance analysis in the egadi islands marine protected area: a mediterranean case study. Mar Policy 2016.
[33] Moscoloni C, Ferrara D, Giglio E, Novo R, Mattiazzo G. Clean energy for eu islands: escape. favignana, levanzo and marettimo, italy. Technical report, ESCAPE – Clean Energy Transition Agenda for the Egadi Archipelago; 2023.
[34] EU parliament. Establishing a framework for community action in the field of marine environmental policy (marine strategy framework directive). 2008 Jun 17.
[35] LibertyLines. Libertylines website; 2024.
[36] Proctor CL, Armstrong LVH. Diesel engine; 2025.
[37] Russel PA, Jackson L, Morton TD. General engineering knowledge for marine engineers. 1986.
[38] Lakshminarayanan PA, Agarwal AK. Design and development of heavy duty diesel engines. 2019.
[39] Feng R, Yu J, Shu X, Deng B, Hua Z. Can the world harmonized steady cycle (whsc) accurately reflect real-world driving conditions for heavy-duty diesel engine emission valuations? a compriensive experimental study. Therm Sci Eng Prog 2025.
[40] U.S. Energy Information Administration. Carbon dioxide emissions coefficients; 2024.
[41] Wartsila. Electric shipping and hybrid ships; 2025.
[42] Hughes A, Drury B. Electric motors and drives. 2019.
[43] Qazi BS, Venugopal P, Rietveld G, Soeiro TB, Shipurkar U, Grasman A, et al. Powering maritime challenges and prospects in ship electrification. IEEE Electrification Mag 2023.
[44] Morace F, Ruggiero V. Comparative test in design of hydrofoils for a new generation of ships. Technol Sci Ships Future 2018.
[45] Carlton JS. Marine propellers and propulsion. 2018.
[46] MAN. Basic principles of ship propulsion. Technical report, MAN Energy Solutions; 2023.
[47] Stapersma D, Woud HK. Beyond matching notes on small craft propulsion applications. J Mar Eng Technol 2014.
[48] Barry CD. Matching propulsion engine with propulsor. In: SNAME/IBEX 2019 Symp 2019.
[49] Williams JW, Olling DS, Merrit RG. Propeller drivers for hydrofoil ships. The Boeing Company; 1984.
[50] Godø JMK, Steen S, Faltinsen OM. A resistance model for hydrofoil fast ferries with fully submerged foil systems. Ocean Eng 2024.
[51] OMEC Motors. Electric motors catalogue. 2024.
[52] Cerdas F, Titscher P, Bognar N, Schmuch R, Winter M, Kwade A, et al. Exploring the effect of increased energy density on the environmental impacts of traction batteries: a comparison of energy optimized lithium-ion and lithium-sulfur batteries for mobility applications. Energies 2018.
[53] Rosenberg J, Walter T, Klysner M, Billeso MB. Retrofit of an existing roro ferry with a hydrogen-electric propulsion system. 2023 Dec 15.
[54] Yu M, Wang K, Vredenburg H. Insights into low-carbon hydrogen production methods: green, blue and aqua hydrogen. Int J Hydrogen Energy 2021.
[55] European Commission. Weekly oil bulletin. 2024 Jul 4.
[56] Bompard E, Botterud A, Corgnati S, Huang T, Jafari M, Leone P, et al. An electricity triangle for energy transition: application to Italy. Appl Energy 2020.
[57] Energetici GM. Gme - electricity markets summary data, Sep 2024.
[58] IRENA International Renewable Energy Agency. Renewable power generation costs in 2022. 2023.
[59] Perna A, Jannelli E, Di Micco S, Romano F, Di Micco S, Minutillo M. Designing, sizing and economic feasibility of a green hydrogen supply chain for maritime transportation. Energy Convers Manag 2023.
[60] Tractebel Engineering S.A. Study on early business cases for h2 in energy storage and more broadly power to h2 applications. 2017 Jun.
[61] IEA. Net zero by 2050 - a roadmap for the global energy sector. Technical report, International Energy Agency; 2021.
[62] World Energy Council and EPRI and PwC. Working paper - hydrogen demand and cost dynamics. Technical report, World Energy Council; 2021.
[63] Deloitte Consulting and Advisory. Clean hydrogen partnership study on hydrogen in ports and industrial coastal areas case studies. Technical report, Clean Hydrogen Partnership; 2023.
[64] Wei G, Qu Z, Zhang J, Chen W. Techno-economic analysis of zero/negative carbon electricity-hydrogen-water hybrid system with renewable energy in remote island. Appl Energy 2025.